UNIVERSITY OF PADOVA

Final Project of Wireless Communications
A.A. 2016/17

Simulation of Multipath Fading Channels: Improvements of Jake's Simulator

Guglielmo Camporese 1153533

Matteo Ciprian 1151519

Contents

1 Abstract

Over the last decades the problem of simulating Rayleigh and Rician multi-path fading has been fully investigated. From the initial model proposed Jakes, many studies have dealt with this theme underlying the limits of Jakes' simulator and proposing new methods. The goal of this paper consist in implementing the principal simulator proposed so far and comparing them in terms of reliability with the ideal model. In this work, four different simulators for Rayleigh multi-path fading have been implemented: three based on Sum of Sinusoids (SoS) method and

one based on filtering of i.i.d. Gaussian random variables. In addiction we have also realized a simulator of Rician fading channel based on SoS. All these methods have been tested and the performances evaluated.

2 Introduction

Channel Simulation is an essential step for the implementation and tuning of wireless networks and communications. For example, before the introduction of each mobile communication systems a large number of theoretical and experimental investigations have to be made. These help to understand how existing resources (energy, frequency range, capita etc.) can be used economically with a growing number of users and how reliable, secure data transmission can be provided for the user in a cheap and simple manner. A practical example can be given by "channel coding" testing. In a communication system the decidability of a symbol is strictly connected with the Source to Noise Ratio (SNR) and more generally with the energy of the received symbol. The efficiency of a particular code has to be tested before being implemented in a real system and for this reason the developer needs to simulate the behavior of channel in terms of fading and distortion of the received signal. For these purposes the development of different propagation models is a crucial step to study various scenarios in wireless communications. There are usually three principal phenomenons to consider: *path-loss*, *shadowing* and *scattering*. *Path-loss* can be considered as the dissipation of power that occurs from the transmitter to receiver with the assumption that the attenuation is equally distributed in each direction. When the attenuation is very strong, the signal is blocked. *Shadowing* is caused by obstacles between transmitter and receiver that attenuate signal power absorbing reflecting the incident wave. One of the possible effect of shadowing is named *"scattering"* intended as the process where some forms of radiation, such as light are forced to deviate from a straight trajectory by one or more paths due to localized non-uniformities in the medium through which they pass. In mobile radio communications, the emitted electromagnetic waves often do not reach the receiving antenna directly due to obstacles blocking the line-of-sight path. In fact, the received waves are a superposition of waves coming from all directions due to reflection, diffraction, and scattering caused by buildings, trees or other obstacles. This effect is known as multi-path propagation or multi-path fading. Due to the this phenomenon, the received signal consists of a sum of attenuated, delayed, and phase-shifted replicas of the transmitted signal.
Also the *Doppler effect* has a negative influence on the transmission characteristics of mobile radio channel. Due to the movement of the mobile unit, the Doppler effect causes a frequency shift modifying the phase of the signal , and, the angle of arrival alpha, which is defined by the direction of arrival of the n-th incident wave and the direction of motion of the mobile unit. Rayleigh and Rician models are the two most important statistical models which describes multi-path-fading. In this context the fading envelope experimented by the channel is viewed as an aleatory process with fixed statistical properties. This work aims at realizing some simulators proposed so far in the literature which are used to simulate fading processes with the two cited statistics. Although there are plenty of techniques proposed, these ones can be grouped in two principal set: *Sum of Sinusoids* [1], [2], [3] , and *Filter-based simulation* [4] which are fully discussed in section 3.3. As reminder, in chapter 3 the objectives and the theoretical basis of Rayleigh and Rician models are explained more in details (sections 3.1 and 3.2); section 3.4 deals with the complications founded during the work while in chapter 4 all the results are given. Finally the conclusions are presented in chapter 5.

3 Technical Approach

3.1 Objectives

As discussed in the introduction 2, wireless multi-path fading phenomenons are usually described with Rayleigh and Rician aleatory processes depending on the experimental scenario (fully discussed in 3.2). In this respect the real challenge lies in finding a method to originate such processes respecting their own statistics with the least computational effort. One of the first work in this direction was produced by Jake [1] during '60 years. His simulator, *Jake's Simulator*, had been used for many years for simulating Rayleigh multi-path fading. Over the last decades, many studies have used new methods [2] - [3], underlying the principal limits of Jake's Simulator in terms of reliability.
This paper aims at making a comparison among all the most known improvements of Jake's simulator. Specifically, the simulators considered in this paper are the following:

- **Rayleigh fading model**: Pop-Beaulieu [2] and Xiao-zheng simulators in respect of *Sum of Sinusoids* method and Kominakis work [4] for what concerns *Filter-based method*.
- **Rician fading model**: the work of Xiao, Zheng and Beaulieu. [5].

3.2 Diagrams/Scenario

If the propagation delay differences among the scattered signal components at the receiver are negligible compared to the symbol interval, then, the channel is said to be frequency-nonselective. In this case, the fluctuations of the received signal can be modeled by multiplying the transmitted signal with an appropriate stochastic model process. After extensive measurements of the envelope of the received signal in urban and suburban areas, i.e., in regions where the line-of-sight component is often blocked by obstacles, the Rayleigh process was suggested as suitable stochastic model. Otherwise, if there is a line-of-sight between the transmitter and the receiver, Rician model is more suitable. To better explain what this means, let $g(t)$ the impulsive response of the channel we want to characterize. It is possible to write it as the sum of quadrature and in-phase term: $g(t) = g_c(t) + jg_s(t)$, where $g_c(t)$ and $g_s(t)$ are two Gaussian process with 0 mean and σ^2 variance. Under the condition of isotropic scattering (the angle of arrival of the scattered signals are uniformly distributed over the interval $[-\pi, \pi]$)) it is possible to show that the fading module $Z = |g(t)|$ and phase $\Theta(t) = \angle g(t)$ are distributed as follows:

$$p_Z(z) = \frac{z}{\sigma^2} e^{-\frac{z^2}{2\sigma^2}} \qquad z \geq 0 \tag{3.1}$$

$$p_\Theta(\theta) = \frac{1}{2\pi} \qquad \text{for } \theta \in [-\pi, +\pi] \tag{3.2}$$

where 3.1 is a Rayleigh distribution. The second-order statistics, the autocorrelation and cross-correlation functions of $g(t)$, are summed-up in the following expressions:

$$R_{g_c,g_c}(\tau)=E[g_c(t)g_c(t+\tau)]=J_0(2\pi f_d\tau) \tag{3.3}$$

$$R_{g_s,g_s}(\tau)=J_0(2\pi f_d\tau) \tag{3.4}$$

$$R_{g_c,g_s}(\tau)=0 \tag{3.5}$$

$$R_{g_s,g_c}(\tau)=0 \tag{3.6}$$

$$R_{g,g}(\tau)=E[g(t)g^*(t+\tau)]=J_0(2\pi f_d\tau) \tag{3.7}$$

$$R_{|g|^2|g|^2}(\tau)=4+4J_0^2(2\pi f_d\tau) \tag{3.8}$$

where the $J_0(\cdot)$ is the zero-order Bessel function and f_d is the maximum Doppler frequency, which depends on the speed of receiver. Differently, if in the channel experiments a line-of-sight, the fading process can be written as $g'(t) = g(t) + m(t)$ where $m(t)$ is the line of sight component and $g(t)$ is the same process described before. Being $\rho = |m(t)|$ it is possible to prove that the magnitude of $Z' = |g'(t)|$ follows a Rician distribution [6] :

$$p_{Z'}(z)=\frac{z}{\sigma^2}e^{-\frac{(z^2+\rho^2)}{2\sigma^2}}I_0(\frac{z\rho}{\sigma^2}) \tag{3.9}$$

where $I_0(\cdot)$ is the modified Bessel function.
The reliability of each simulation model will be evaluated comparing the first and second order statistics of the fading process originated by the simulation with the ideal ones 3.3. Other metrics such as AFD and LCR will be used in our work; a complete explanation of these metrics will be given in paragraph 3.3.1.

3.3 Mathematical Models Used

3.3.1 Simulation of Rayleigh Channel

Jake's Simulator As discussed before, Jake's simulator is one of the first work which realizes a proper simulation of a wireless Rayleigh multi-path channel. In developing his simulator, Jake starts with an expression representing the received signal as a superposition of waves, similar to that given by Bello (the path delays is set equal to zero, $\tau_n = 0$):

$$g(t)=E_0\sum_{n=1}^{N}C_n e^{j(2\pi f_d t cos(\alpha_n)+\phi_n)} \tag{3.10}$$

where E_0 is a scaling constant, C_n, α_n and ϕ_n are, respectively, the random path gain, angle of incoming wave, and initial phase associated to the n-th propagation path, and f_d is the maximum Doppler frequency occurring when $\alpha_n = 0$. Based on Clarke's reference model [7], Jakes derived his well-known simulation model for Rayleigh fading channel imposing the following conditions:

$$C_n=\frac{1}{\sqrt{N}}, \qquad \alpha_n=\frac{2\pi n}{N}, \qquad \phi_n = 0 \qquad n = 1, 2, ...N \tag{3.11}$$

The normalized low-pass fading process of this model is given by :

$$u(t)=u_c(t)+ju_s(t) \tag{3.12}$$

$$u_c(t)=\frac{2}{\sqrt{N}}\sum_{n=0}^{M}a_n cos(w_n t) \tag{3.13}$$

$$u_s(t)=\frac{2}{\sqrt{N}}\sum_{n=0}^{M}b_n cos(w_n t) \tag{3.14}$$

$$\tag{3.15}$$

where $N = 4M + 2$, and:

$$a_n = \begin{cases} \sqrt{(2)}cos\beta_0, n = 0 \\ 2cos\beta_n, n = 1, 2....M \end{cases} \quad (3.16) \qquad b_n = \begin{cases} \sqrt{(2)}sin\beta_0, n = 0 \\ 2sin\beta_n, n = 1, 2....M \end{cases} \quad (3.17)$$

$$\beta_n = \begin{cases} \frac{\pi}{4}, n = 0 \\ \frac{\pi n}{M}, n = 1, 2....M \end{cases} \quad (3.18) \qquad w_n = \begin{cases} w_d, n = 0 \\ w_d cos\beta_n, n = 1, 2....M \end{cases} \quad (3.19)$$

These simplifications makes the simulator deterministic because once the number of sinusoids (N) and the Doppler frequency are fixed, the other parameters can be completely calculated. The worst consequence derives from the fact that $g(t)$ process is not *wide sense stationary* as it should be for satisfying Rayleigh process property. Anyway, this simulator has been used for years for its simplicity and low computational effort.

A first improvement: Pop-Beaulieu simulator Among the Jakes simulator family, a new improved model proposed by Pop and Beaulieu is worthy of mention due to its wide-sense stationarity [2]. In this case the low-pass fading process is given by sum of sinusoids as in Jakes' but a random phase is introduced:

$$u(t)=u_c(t)+ju_s(t) \quad (3.20)$$

$$u_c(t)=\frac{2}{\sqrt{N}}\sum_{n=0}^{M} a_n cos(w_n t+\phi_n) \quad (3.21)$$

$$u_s(t)=\frac{2}{\sqrt{N}}\sum_{n=0}^{M} b_n cos(w_n t+\phi_n) \quad (3.22)$$

$$(3.23)$$

where a_n, b_n, β_n and w_n are the same as those of Jakes' original model given by 3.12 and ϕ_n are independent random variables uniformly distributed on $[-\pi, \pi)$ for all n.
Although this approach solves the problem of the stationarity, some problems with higher-order statistics remain. As fully explained in [2] the autocorrelations and cross correlations of the quadrature components and the autocorrelation of the squared envelope of the improved simulator fail at matching the desired statistics.

Xiao-Zheng simulator In order to overcome the problems present in the simulation model of Pop-Bealeiau, a new simulator has been proposed by Xiao and Zheng [3]. Similar to the previous ones, Xiao-Zheng simulator is based on sum-of-sinusoids paradigm but in this case all three parameters C_n, α_n and ϕ_n are set as random variables. To properly introduce randomness we consider the following simulation prototype function:

$$g(t)=E_0\sum_{n=1}^{N} C_n e^{(j(2\pi f_d t cos(\alpha_n)+\phi_n))} \quad (3.24)$$

where the parameters are set in the following way:

$$C_n=\frac{exp(j\psi_n)}{\sqrt{N}} \qquad \alpha_n=\frac{2\pi n-\pi+\theta}{N} \qquad n = 1, 2, ...N \quad (3.25)$$

$$\phi_n=-\phi_{\frac{N}{2}+n}=\phi \qquad n = 1, 2, ...\frac{N}{2} \quad (3.26)$$

$$(3.27)$$

and ψ_n, θ, ϕ are independent random variables uniformly distributed on $[-\pi, \pi]$. Moreover, differently from the Jakes' procedure $\psi_{\frac{N}{2}+n} = \psi_n$. Fixing $\frac{N}{4} = M$ and $w_n = w_d cos\alpha_n$, some simplifications can be done on the formula 3.24 and it is possible to reduce the normalized low-pass fading process at this expression :

$$u(t)=u_c(t)+ju_s(t) \tag{3.28}$$

$$u_c(t)=\frac{2}{\sqrt{M}}\sum_{n=1}^{M} cos(\psi_n)cos(w_d tcos(\alpha)t+\phi) \tag{3.29}$$

$$u_s(t)=\frac{2}{\sqrt{M}}\sum_{n=1}^{M} sin(\psi_n)cos(w_d tcosa(\alpha)+\phi) \tag{3.30}$$

$$\tag{3.31}$$

where the term $\alpha_n = \frac{2\pi n-\pi+\theta}{N}$ for $n = 1, 2, ..M$. In [3], the second order statistics of the normalized low-pass fading process 3.28 are calculated. In the following, results are reported:

$$R_{u_c,u_c}(\tau)=J_0(2\pi f_d\tau) \tag{3.32}$$

$$R_{g_s,u_s}(\tau)=J_0(2\pi f_d\tau) \tag{3.33}$$

$$R_{u_c,u_s}(\tau)=0 \tag{3.34}$$

$$R_{u_s,u_c}(\tau)=0 \tag{3.35}$$

$$R_{u,u}(\tau)=J_0(2\pi f_d\tau) \tag{3.36}$$

$$R_{|u|^2|u|^2}(\tau)=4+4J_0^2(2\pi f_d\tau)+\frac{4+2J_0^2(2\pi f_d\tau)}{M} \tag{3.37}$$

Comparing with the ideal model, Xiao-Zheng simulator succeeds in reaching better performance about the second-order statistics; nevertheless it approaches the fourth-order statistic $R_{|u|^2|u|^2}(\tau)$ only asymptotically

A filter-based approach: Komninakis' simulator Different from the *Sum of Sinusoids* approach, in [4] a new method is explicated to simulate $g(t)$. In this paper, for practice, this method will be called *Filter-based approach*. It adopts the filtering of independent Gaussian random variables through an IIR filter with a particular frequency-response that will be explicated in the following lines. As shown in 3.3, the autocorrelation of the Rayleigh process $g(t)$ is given by the zero-order Bessel function. Its transform (the PSD) is expressed by the following expression:

$$S_{gg}(f)=\begin{cases}\frac{1}{\pi f_d}\frac{1}{\sqrt{1-\frac{f}{f_d}^2}}, |fd| < f_d \\ 0, \text{otherwise}\end{cases} \tag{3.38}$$

According to this procedure the IIR filter has to approach the square root of 3.38, $H(f) = \sqrt{S_{gg}(f)}$ because, since the filter operates only linear operations on the input sequence of Gaussian random variables, the output sequence remains Gaussian. Moreover, the relationship between the input and output spectral density are linked by the well-known formula $S_{out}(f) = S_{in}(f)|H(f)|^2$. If the input sequence is independent (flat PSD), the spectral shape of PSD of the output Gaussian sequence will follow 3.38, as desired. Given that this expression 3.38 is irrational, one of the main challenge consists in creating the filter with a frequency response that approaches it. As reported in [4], the filter is designed with an iterative optimization algorithm described in [8] which allows to obtain an IIR filter with arbitrary magnitude response. Another problem is caused by the fact that the maximum Doppler frequency is small compared to the sampling frequency f_c : $f_d << f_c$. Consequently, the rate $\rho = \frac{f_d}{f_c}$ is very low and the filter results extremely narrow-band conducting to an impractical filter-response with a very sharp cutoff and infinite attenuation in the stop-band. This problem is solved designing the filter with a larger band limitation (for instance in this paper we set $\rho = 0.2$) and interpolating the filtered signal with a polyfase interpolator.

3.3.2 Simulation of Rician Channel

Most of the theoretical instruments dealt for simulating Rayleigh multi-path fading can be exploited for the simulation of Rician multi-path fading where there is a line of sight between the transmitter and receiver. In this report, it is considered the work developed in paper [5], where a new reference simulation model based on *Sum of Sinusoids* is introduced. At first, the authors present a new improved version of Rayleigh simulator similar to the one presented in [3]. Specifically the normalized low-pass process is written as following:

$$u(t)=u_c(t)+ju_s(t) \tag{3.39}$$

$$u_c(t)=\frac{1}{\sqrt{N}}\sum_{n=1}^{N} cos(w_d t cos(\alpha_n)+\phi_n) \tag{3.40}$$

$$u_s(t)=\frac{1}{\sqrt{N}}\sum_{n=1}^{N} cos(w_d t cos(\alpha_n)+\phi_n) \tag{3.41}$$

$$\tag{3.42}$$

with $\alpha_n = \frac{2\pi n+\theta_n}{N}$ for $n = 1, 2, ..N$, and ϕ_n θ_n independent and uniformly distributed $[-\pi, \pi)$ for all n. Starting from this model, the Rician low-pass process $z(t)$ is obtained adding the LoS component i.e. :

$$z(t)=z_c(t)+jz_s(t) \tag{3.43}$$

$$z_c(t)=\frac{u_c(t)+cos(w_d t cos(\theta_0)+\phi_0)}{\sqrt{1+K}} \tag{3.44}$$

$$z_s(t)=\frac{u_s(t)+cos(w_d t sin(\theta_0)+\phi_0)}{\sqrt{1+K}} \tag{3.45}$$

$$\tag{3.46}$$

where K is the ratio of the specular power to scattered power, θ_0 and ϕ_0 are the angle of arrival and the initial phase, respectively, of the specular component. ϕ_0 is a random variable uniformly distributed over $[-\pi, \pi)$. Having this simulation model the authors of [5] calculate also the theoretical distribution of Rician fading:

$$p_Z(z)=2(1+K)ze^{-K-(1+K)z^2}J_0(2z\sqrt{K(1+K)}) \qquad \text{for } z \geq 0 \tag{3.47}$$

$$p_\Theta(\theta)=\frac{1}{2\pi} \qquad \text{for } \theta \in [-\pi, +\pi] \tag{3.48}$$

3.3.3 Metrics for performances evaluation

As briefly anticipated in the previous paragraphs each simulator will be evaluated according to three criteria. The first one is how the density function of the generated process well approaches the theoretical one (eq. 3.1 3.9) while, secondly, the same comparison is done between the second order statistics ($R_{g_c,g_c}, R_{g_c,u_s}, ecc..$). As third step, LCR and AFD metrics are introduced. This two functions are respectively the rate at which the envelope crosses a specified level in the positive slope and the average time duration that the fading envelope remains below a specified level. The calculation of LCR for a specific level R results from the following integral: $LCR = \int_0^\infty rp(R, r)dr$. For Rayleigh fading it can be expressed in a closed form: $LCR(\rho) = \sqrt{2\pi} f_d \rho e^{-\rho^2}$ where $\rho = R/R_{rms}$ and R_{rms} is the root mean-square of the levels, while AFD is given by the formula $AFD(\rho) = \frac{e^{\rho^2}-1}{\rho f_d \sqrt{\pi}}$. For what concerns Rician fading, these metrics cannot be obtained in a closed form. However, in [5] , the authors have calculated the expression to obtain them:

$$LCR(\rho)=\sqrt{\frac{2(1+K)}{\pi}} f_d e^{-K-(1+K)\rho^2} \int_0^\pi ([1+\frac{2}{\rho}\sqrt{\frac{K}{1+K}}cos^2(\theta_0)cos\alpha]exp[2\rho\sqrt{K(1+K)}cos\alpha - 2Kcos^2\theta_0 sin^2\alpha])d\alpha \tag{3.49}$$

$$AFD(\rho)=\frac{1-Q[\sqrt{2K},\sqrt{2(1+K)\rho^2}]}{LCR(\rho)} \tag{3.50}$$

where $Q(\cdot,\cdot)$ is the first order Marcum-function. Having evaluated all these points, the better is the simulator the more LCR and AFD theoretical functions are approximated (in function of ρ).

3.4 Complications Found

One of the most difficult part of this work lies in finding the informations. Despite the papers are written in a clear way, sometimes, the authors are not able to convey directly the real goals of channel simulation and they do not succeed in giving an overview. We have tried to compensate this lack in the introduction, exposing step-by-step the whole theoretical background which precedes the use of these simulators. In our opinion this is compulsory for drawing up a paper which can be considered "autonomous", helping the reader in understanding the work.
From a more practical point of view, the use of the Matlab framework for reporting and plotting the results in the charts is a little tedious.

4 Results

4.1 Zheng-Xiao

4.1.1 Performance Evaluation

The performances of the simulator proposed in Fig.4.1-4.5 is now compared with the mathematical reference model previous discuss in 3.2. In the implementation, the parameter related to the number of sinusoids M is fixed to $M = 8$ and the normalized maximum Doppler frequency is fixed to $f_dT = 0.025$. The overall performances are then evaluated on the average of $N_{stat} = \{10, 50, 100\}$ random trials.

4.1.2 Evaluation of Correlation Statistics

A comparison between the ideal channel and the simulated channel about the second order statistics is now presented. As can be seen from Figs.4.1-4.3, the simulation results show that the autocorrelations of the quadrature components and the complex envelope and the cross correlations of the quadrature components match the desired ones very well, even though M is as small as 8, and the number of statistical trials is as low as $N_{stat} = 50$. The autocorrelation of the squared envelope is similar to the ideal statistic when $M = 8$ but with bigger values of M the comparison gets better. If we increase the number of statistical trials N_{stat} the difference between all the simulated statistics and the ideal statistics decrease. This result is completely predicted by the theoretical calculations made in [3] and reported in 3.32.

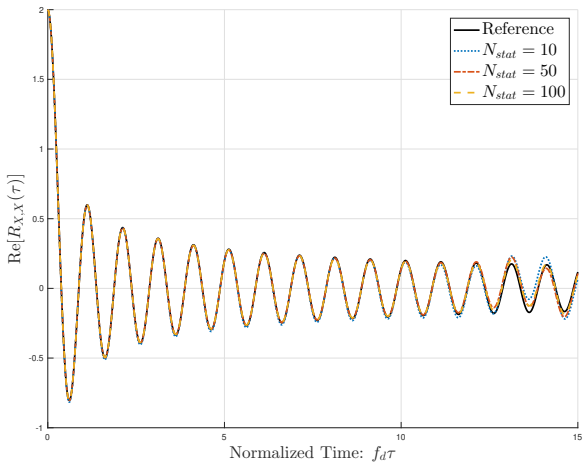

(a) Real part of the autocorrelations of the simulated complex fading $X(t)$ and reference $g(t)$.

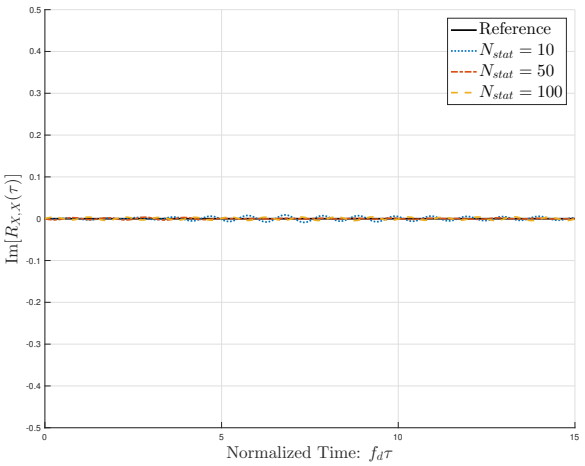

(b) Imaginary part of the autocorrelations of the simulated complex fading $X(t)$ and reference $g(t)$.

Figure 4.1: Xiao-Zheng simulator results.

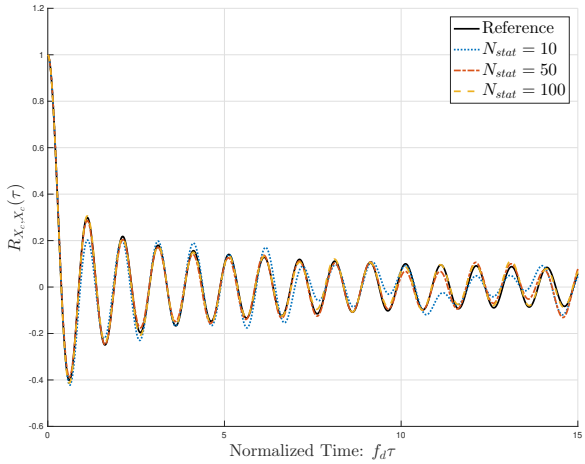

(a) Autocorrelations of the simulated real-part fading $X_c(t)$ and reference $g_c(t)$.

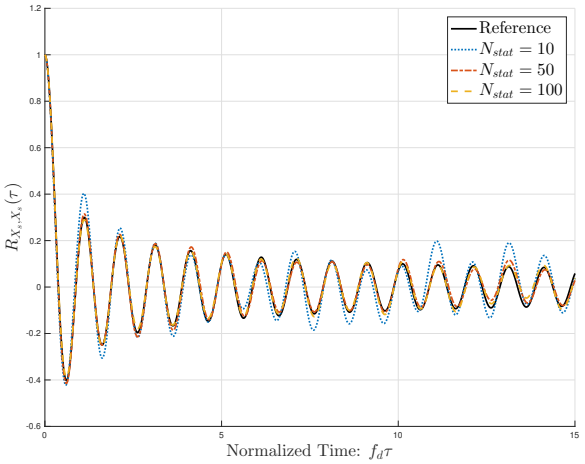

(b) Autocorrelations of the simulated imaginary-part fading $X_s(t)$ and reference $g_s(t)$.

Figure 4.2: Xiao-Zheng simulator results.

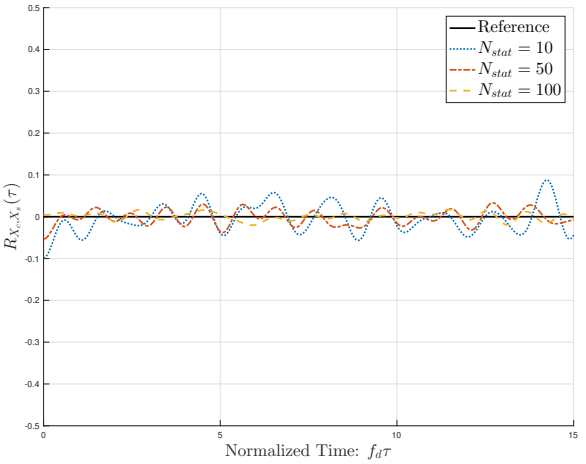

(a) Cross correlations of the simulated quadrature components of the fading envelope $|X(t)|$ and reference $g(t)$. In this simulation the plot of $R_{X_sX_c}(\tau)$ is omitted because it is almost identical to $R_{X_cX_s}(\tau)$.

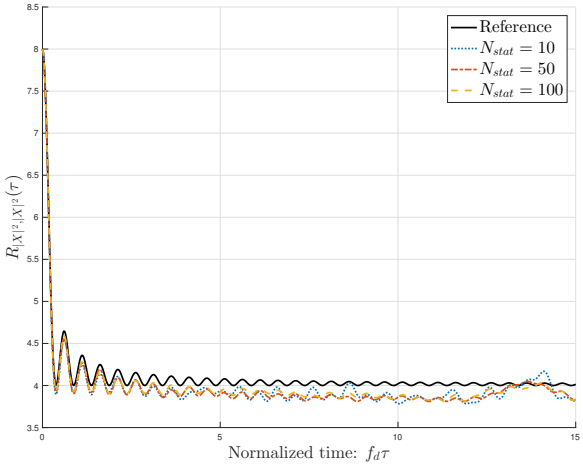

(b) Autocorrelations of the simulated squared envelope $|X(t)|^2$ and reference $|g(t)|^2$.

Figure 4.3: Xiao-Zheng simulator results.

4.1.3 Evaluation of PDFs of the Envelope and Phase

In the Fig.4.4 there are the PDF of the fading envelope (Fig.4.4a) and the PDF of the phase (Fig.4.4b) of the simulated channel. It can be seen that the PDF of the envelope matches very well the ideal ones given in 3.2, also when the number of trials is small ($N_{stat} = 10$). In the case of the PDF of the phase, however there is less match with the ideal model but things get better both when the number of trials N_{stat} increase and when $M > 8$.

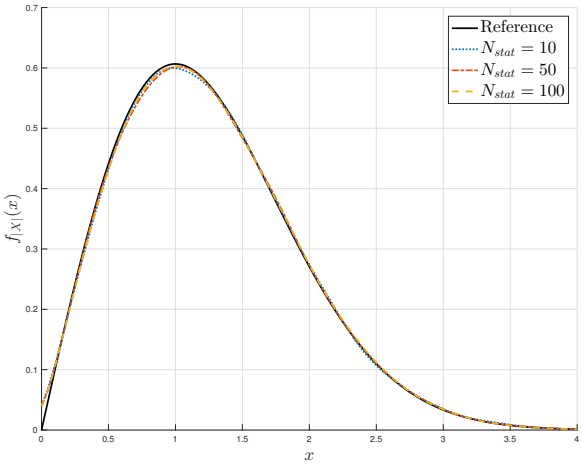

(a) PDFs of the simulated fading envelope $|X(t)|$ and reference $|g(t)|$.

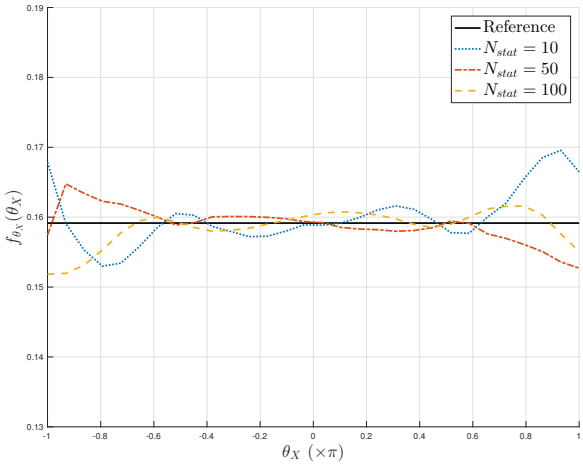

(b) PDFs of the simulated fading phase $\theta_X(t)$ and reference $\Theta_g(t)$.

Figure 4.4: Xiao-Zheng simulator results.

4.1.4 Evaluation of the LCR and the AFD

In the Fig.4.5, it is shown the normalized level crossing rate $L_{|X|}/f_d$ (Fig.4.5a) and the normalized average fade duration $T_{|X|}f_d$ (Fig.4.5b) of the channel for various statistical trials $N_{stat} = \{10, 50, 100\}$. It can be seen that the simulated measurements agree very well with the ideal ones even if N_{stat} is small.

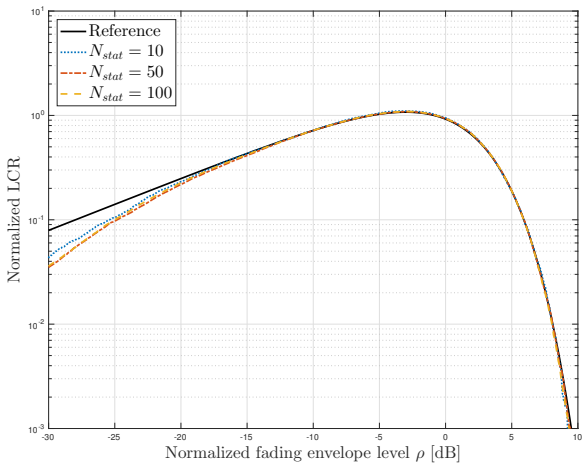

(a) LCRs of the simulated fading envelope $|X(t)|$ and reference $|g(t)|$.

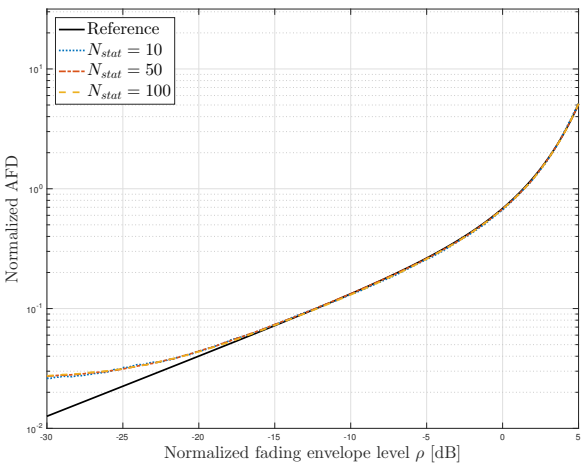

(b) AFDs of the simulated fading envelope $|X(t)|$ and reference $|g(t)|$.

Figure 4.5: Xiao-Zheng simulator results.

4.2 Komninakis

4.2.1 Performance Evaluation

For the filter based simulator proposed by Komninakis in [4] we use the Ellipsoid optimization algorithm in a way to ensure the squared envelope of the filter's frequency response equal to the target PSD described in 3.38. Following the indications in [4], the filter has been designed with 501 frequency points, $K = 7$ biquads and the normalized maximum Doppler frequency $f_d T = 0.2$.

4.2.2 Evaluation of Filter Design and Correlation Statistics

In Fig. 4.6a there is the comparison between the ideal and the simulated square envelope frequency response of the designed filter and, as in [4], they match very well. In this simulation, the required normalized maximum Doppler frequency is $f_d T = 0.05$ so at the output of the filter the signal has been interpolated by a factor of 4. As shown in Fig. 4.6b, the real part and the imaginary part of the autocorrelation of the complex impulse response approaches the theoretical one very well.

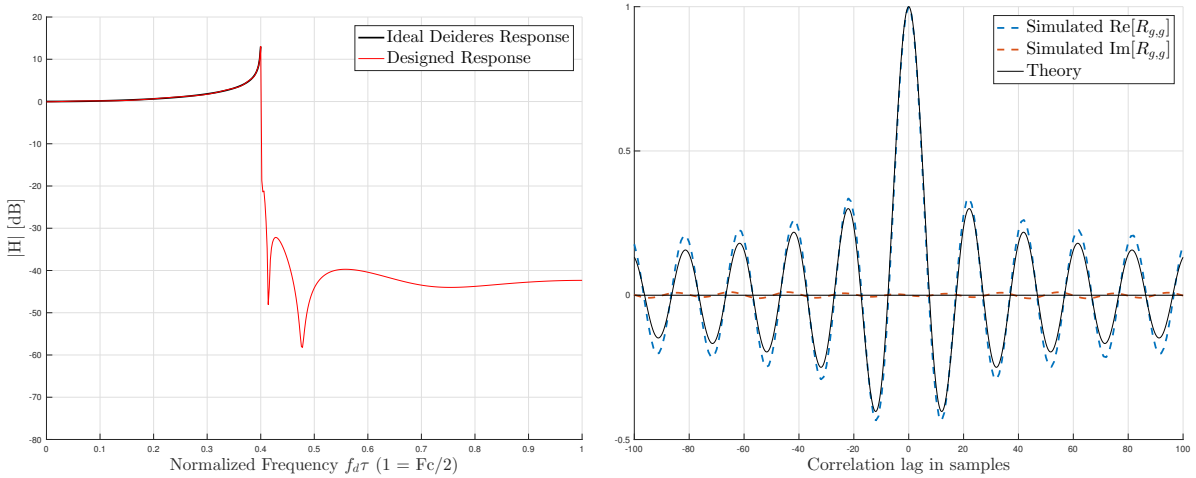

(a) Magnitude frequency response for the designed filter overlayed against the desired theoretical response.

(b) Real and imaginary part of the autocorrelation function of the sampled Rayleigh fading waveform plotted against theoretical Bessel autocorrelation.

Figure 4.6: Komninakis simulator results.

4.2.3 Evaluation of the LCR

In Fig.4.7 it is reported the comparison between ideal and simulated level crossing rate for different maximum doppler frequency $f_d T = \{0.5, 0.01, 0.002\}$ which correspond to different interpolating factor for the filtered channel $I = \{4, 20, 100\}$. The LCR is plotted in relation to the normalized level $\lambda = R/R_{rms}$ expressed in dB where R is the level. It can be seen that the ideal function and the simulated one fit correctly for large values of λ.

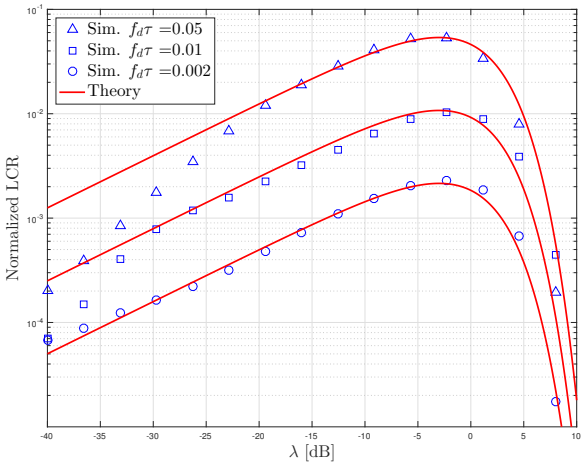

(a) Level crossing rate of the amplitude of the sample Rayleigh fading waveform.

Figure 4.7: Komninakis simulator results.

4.3 Rician

4.3.1 Performance Evaluation

Verifying the accuracy of the simulated channel is carried out by comparing the simulation with finite number of sinusoids N and the infinite number of sinusoids N of the theoretical model. The results below are done with $N = 8$ but it is reasonable that with larger value of N the statistical accuracy of the simulator increases. The simulation has been performed following the indications of [5]: the angle of arrival $\theta_0 = \pi/4$ and $\theta_0 = 0$ only for the evaluation of the AFD, the maximum Doppler set to $f_dT = 0.01$ and for the power LoS/non-LoS ratio K the sequence $K = \{0, 1, 3, 5\}$ is used. All the statistical performances are then evaluated averaging over $N_{stat} = 100$ random trials.

4.3.2 Evaluation of Correlation Statistics

In Fig. 4.8-4.9, there are represented the real and imaginary part of the autocorrelation of the complex envelope and the autocorrelation of the squared envelope respectively. In all this figures the simulated data match the theoretical ones for all values of K, in particular in this case for $K = \{0, 1, 3\}$, even if N is small.

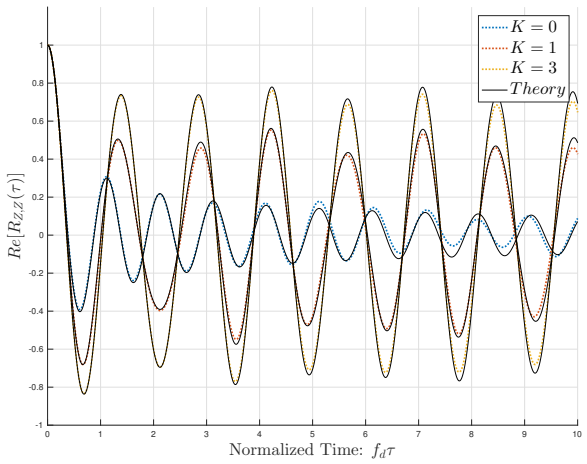

(a) The real part of the autocorrelation of the complex envelope $Z(t)$ with $\theta_0 = \pi/4$ for $K = 1$ and $K = 3$ Rician cases.

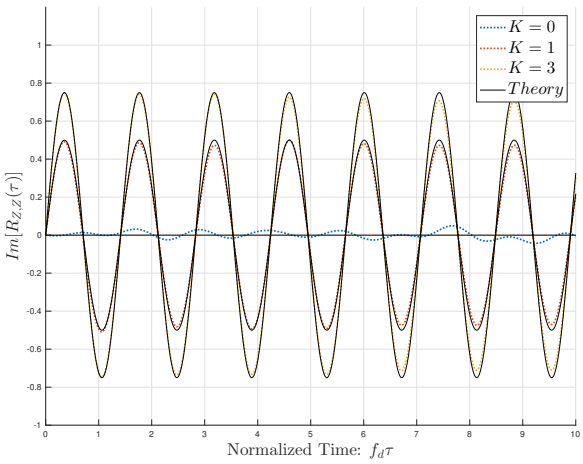

(b) The imaginary part of the autocorrelation of the complex envelope $Z(t)$ with $\theta_0 = \pi/4$ for $K = 1$ and $K = 3$ Rician cases.

Figure 4.8: Xiao-Zheng-Beaulieu simulator results.

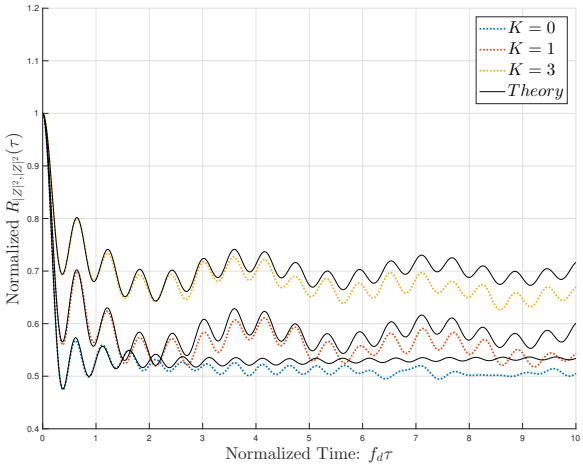

(a) The autocorrelation of the squared envelope $|Z(t)|^2$ with $\theta_0 = \pi/4$ for $K = 1$ and $K = 3$ Rician cases.

Figure 4.9: Xiao-Zheng-Beaulieu simulator results.

4.3.3 Evaluation of PDFs of the Envelope and Phase

In the figures below there are the evaluation for the PDF of the envelope (Fig. 4.10a) and for the PDF of the phase (Fig 4.10b) for different values of K, in particular for $K = \{0, 1, 3, 5, 10\}$ and averaging over $N_{stat} = 100$ random trials. It can be seen that the simulated PDFs match very well to the theoretical ones even if N is small.

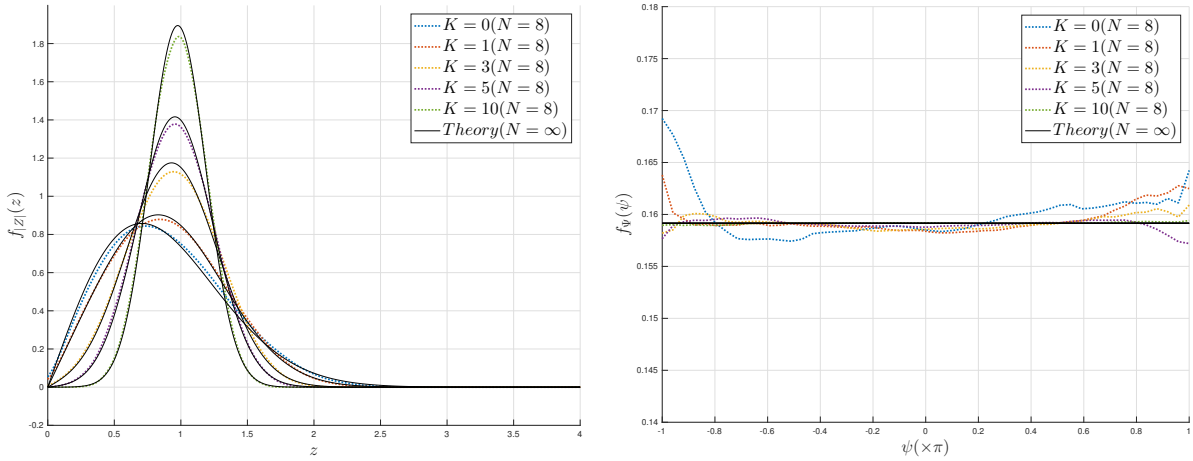

(a) The PDF of the fading envelope $|Z(t)|$.

(b) The PDF of the fading phase $\Psi(t)$.

Figure 4.10: Xiao-Zheng-Beaulieu simulator results.

4.3.4 Evaluation of the LCR and AFD

In the graphs below there are the simulated and theoretical normalized level crossing rate $L_{|Z|}/f_d$ Fig. 4.11a and normalized average fading duration $T_{|Z|}f_d$ (Fig. 4.11b). All the simulation is done for different values of K in particular for $K = \{0, 1, 3, 5, 10\}$ and averaging over $N_{stat} = 100$ statistical trials. It can be seen that the simulated values agree very well with the theoretical references for LCR and AFD given in 3.49 even if N is small.

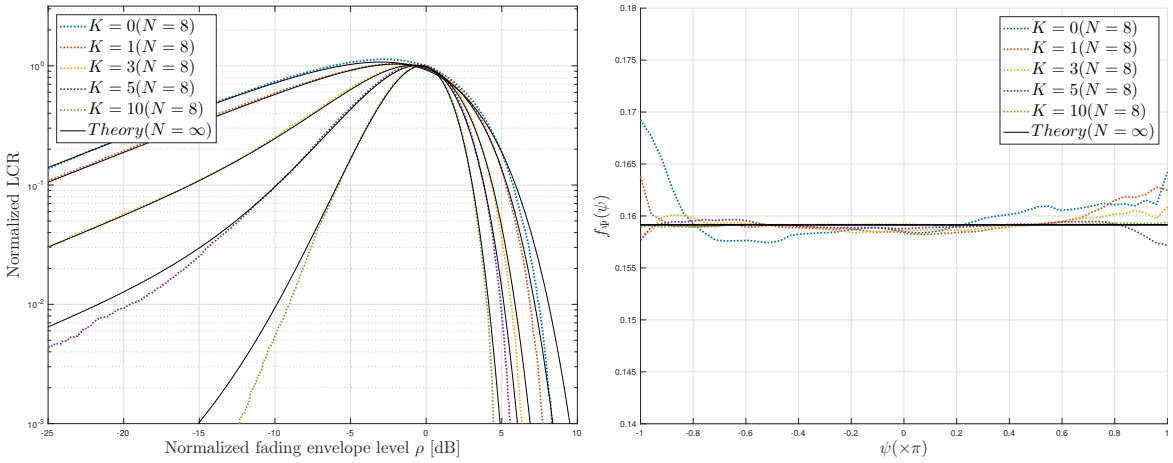

(a) The normalized LCR of the fating envelope $|Z(t)|$, where $\theta_0 = \pi/4$ for all $K > 0$ Rician fading.

(b) The normalized AFD of the fating envelope $|Z(t)|$, where $\theta_0 = 0$ for all $K > 0$ Rician fading.

Figure 4.11: Xiao-Zheng-Beaulieu simulator results.

5 Conclusions

In this project it has been implemented and tested the performances of some simulators for Reyleigh and Rician channels, proposed in [3], [4], [2], [5]. The performances are evaluated comparing the statistical properties of the simulated fading process with the reference statistic. Many

of the simulators in this work are based on the Jakes' work and each one improves the basic idea proving the gain mathematically and by simulation. In particular, *Xiao and Zheng simulator* reaches very good performances, approaching totally the ideal second order statistics as the number of trials increases. Some errors are still observable regarding the density function of the phase of the fading process and the autocorrelation of the squared module of the fading. For what concerns *Komninakis simulator* [4], Filter-based method, the Ellipsoid algorithm proposed in [8] approximates the filter's response optimally. The second order statistics follow almost perfectly the ideal ones but LCR function is not approached as well as in case of Xiao-Zheng simulator. On the other hand, from a computational point of view, the simulation process proposed by Komninakis seems to require a lower computational efforts: when the filter is created, the algorithm has just to realize the filtering and interpolating process which result faster than the super-position of sinusoids as overall.
Rician simulator, [5], gets good results as well. Being the simulation model very similar to the one proposed by Xiao-Zheng, it shows the same lack: the autocorrelation of the squared module of the fading and the density function of the phase do not fit completely the reference functions.
In this project we have learn how a wireless channel simulator works, coding it from scratch. We have also understand how to evaluate their performances and we have improved our Matlab skills.

Bibliography

[1] W. C. Jakes and D. C. Cox, eds., *Microwave Mobile Communications*. Wiley-IEEE Press, 1994.

[2] M. F. Pop and N. C. Beaulieu, "Limitations of sum-of-sinusoids fading channel simulators," *IEEE Transactions on Communications*, vol. 49, pp. 699–708, Apr 2001.

[3] Y. R. Zheng and C. Xiao, "Simulation models with correct statistical properties for rayleigh fading channels," *IEEE Transactions on Communications*, vol. 51, pp. 920–928, June 2003.

[4] C. Komninakis, "A fast and accurate rayleigh fading simulator," in *Global Telecommunications Conference, 2003. GLOBECOM '03. IEEE*, vol. 6, pp. 3306–3310 vol.6, Dec 2003.

[5] C. Xiao, Y. R. Zheng, and N. C. Beaulieu, "Novel sum-of-sinusoids simulation models for rayleigh and rician fading channels," *IEEE Transactions on Wireless Communications*, vol. 5, pp. 3667–3679, December 2006.

[6] M. Pätzold and M. Pätzold, *Mobile fading channels*. J. Wiley, 2002.

[7] R. H. Clarke, "A statistical theory of mobile-radio reception," *The Bell System Technical Journal*, vol. 47, pp. 957–1000, July 1968.

[8] K. Steiglitz, "Computer-aided design of recursive digital filters," *IEEE Transactions on Audio and Electroacoustics*, vol. 18, pp. 123–129, Jun 1970.